

Optical Wedge Effects in Instruments and Standards for Molecular Absorption Spectrophotometry

JOHN C. TRAVIS,* MELODY V. SMITH, and GARY W. KRAMER

Analytical Chemistry Division, National Institute of Standards and Technology, Gaithersburg, Maryland 20899

The optical wedge of some older, individual solid NIST absorbance filter standards has been found to cause bias in the indicated absorbance readings of certain instruments. In a collimated-beam spectrophotometer, the sample beam is deflected by about half of the wedge angle in the sample. For inverted geometry designs, small deflections can give rise to large changes in the field of view of the entrance slit of the spectrometer downstream from the sample. Beam deflection is also found to induce small apparent wavelength shifts in data taken through a wedged sample, resulting in spectral artifacts derived from spectral features of the system or of an absorbing sample. These spectral artifacts turn out to be robust, and simple cell-reversal difference spectra can provide useful diagnostic indicators of optical wedge. Solid photometric standards are found to be reliable, if manufactured to wedge angles of less than 0.1 mrad. Despite a wedge tolerance of 0.9 mrad in the sealed cuvettes of a wavelength standard, wavelength shifts are shown to be negligible when compared to the stated uncertainties. For normal use, accuracy may be achieved by utilizing the same cell in the same orientation for both background and sample spectra or by hand selection of cells.

Index Headings: Cell; Cuvette; Filter; Optical quality; Optical wedge; Spectrophotometry; Standard Reference Material; UV-visible absorption.

INTRODUCTION

The National Institute of Standards and Technology (NIST) offers Standard Reference Materials (SRMs) for verifying the measurement accuracy and calibrating the wavelength scale of molecular absorption spectrometers (UV-visible spectrophotometers).¹⁻⁵ In spite of the quarter-century history of this activity and the maturity of the measurement method, the program remains under continuous review to accommodate changing needs and to improve both the accuracy and utility of the standards. It has recently been necessary to modify the optical wedge tolerance of solid filter standards to accommodate spectrophotometer configurations based on solid-state array detector technology.

Solid-state detector arrays allow optical spectrometers to monitor a wide range of wavelengths simultaneously, thus producing a "multiplex advantage" with respect to signal-to-noise ratio per unit time. Such "optical multi-channel detection" has become commonplace in many areas of optical spectroscopy. The lure of instantaneous absorption spectra for real-time applications such as chromatography detection, chemical process control, and at-line process monitoring is fueling a steady growth in the installed instrument base for such devices.

NIST was alerted that the optical wedge, the angle between the entry and exit faces, of some individual solid

NIST filter standards was sufficient to cause bias in the indicated absorbance reading of some multichannel instruments.⁶ Investigation into the origins of this effect in sample beam transfer optics and in normal filter construction has led to the tightening of NIST filter specifications and production quality control, as well as some potentially important observations regarding normal cuvette usage, diagnostic measures, and instrument design.

THEORY

Errors in Transmittance and Absorbance. Molecular absorption spectrometry, or UV-visible spectrophotometry, characterizes the fractional absorption of light as a function of wavelength for a sample solution contained in a cell of known pathlength with transparent windows. The sample transmittance at a given wavelength is defined as $T(\lambda) \equiv I(\lambda)/I_0(\lambda)$, where $I(\lambda)$ is the intensity of light at wavelength λ detected through the sample, and $I_0(\lambda)$ is the light intensity incident on the sample at the same wavelength. The electronic proportionality factor between the light intensity and signal response cancels in the ratio, for linear detectors.

Although the transmittance is the quantity experimentally determined, the exponential dependence between transmittance and analyte concentration (given by Beer's law) makes the absorbance, A , defined as $A \equiv -\log(T)$ of more interest to chemists, since this quantity depends linearly upon both pathlength and analyte concentration. Taking the differential of the absorbance/transmittance relationship given above shows that

$$\delta A = -\delta(\log(T)) = -0.434\delta(\ln(T)) = -0.434 \frac{\delta T}{T} \quad (1)$$

such that errors in absorbance scale linearly with *relative errors* in transmittance. Overall uncertainties of 0.5% *relative* in transmittance, or about 0.002 absorbance units (AU) in absorbance, are typical of NIST standards over the 10 to 30% transmittance range.

The instruments discussed herein are "single-beam" instruments, for which two spectral scans or single wavelength measurements are required to complete the transmittance measurement. "Double-beam" instruments split the sampling beam and measure the sample and reference intensities in parallel. Though the discussion and data presented are based on the single-beam design, the extension to the double-beam geometry should be apparent.

In chemical measurements, with the background measurement taken with a cuvette containing a blank solution in the beam, the absorbance obtained is due to the absorption within the sample, and the effects of exterior reflections from the cell-wall-to-air interfaces are canceled in the ratio. In contrast, when a solid filter is used

Received 24 April 1998; accepted 28 July 1998.

* Author to whom correspondence should be sent.

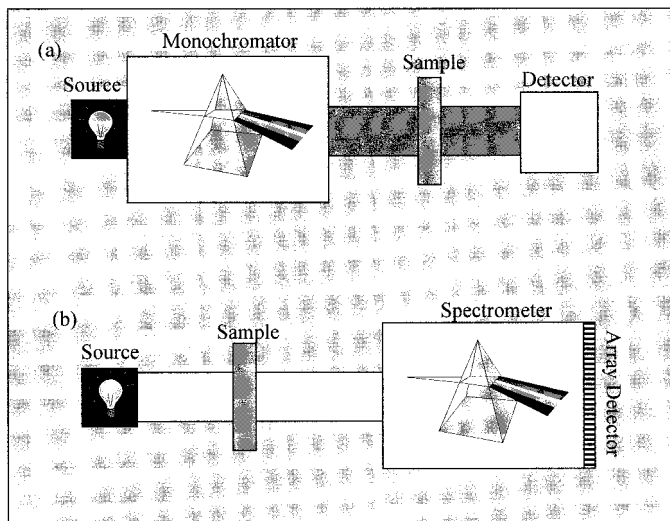


FIG. 1. Two common component arrangements for single-beam UV-visible absorption spectrophotometry. (a) The "normal" configuration has monochromatic light passing through the sample and into the detector. (b) The "inverted" or post-sample dispersion configuration is essential for simultaneous parallel detection.

to verify the accuracy of a spectrophotometer, the background spectrum is obtained with respect to air, and reflection losses from the two surfaces of the filter contribute to the resulting measured transmittance. For this reason, NIST refers to the negative logarithm of this total transmittance as the "transmittance density" as opposed to "absorbance" (the negative log of the "internal transmittance"),⁷ and the SRM certificate advises that the user's instrument should yield absorbance values equivalent to the certified transmittance densities.

In this paper, a number of filter-reversal difference spectra are shown to illustrate the effect of the optical wedge. For such difference spectra, the ordinate is truly an absorbance difference, since the external reflection losses are canceled in the transmittance density difference.

Among other things, the accuracy of the absorption measurement depends greatly upon the extent to which the light beam for the background measurement is identical to that for the sample measurement, with the single exception of its having passed through the sample for the latter. As will be shown below, the optical wedge in a solid standard or measurement cuvette has the potential of deflecting the beam and compromising the measurement in certain circumstances.

Pre- and Post-Filter Dispersion Geometries. Ideally, it is irrelevant whether the light is dispersed before or after passing through the sample, as illustrated by the two optical diagrams shown in Fig. 1. The configuration of Fig. 1a has been broadly adopted over the years and is considered the normal geometry for scanning spectrophotometers. Here the dispersive element is mechanically adjusted, yielding a scan of spectral intensity as a function of wavelength. A known potential for measurement error in normal geometry spectrophotometers is that optical deflection or translation (shear) of the sample beam by wedge or tilt of the sample cuvette or standard may shift the position of the beam on the face of the detector, relative to the reference measurement. Resultant error

may arise from spatial nonuniformity of the sensitivity across the face of the detector. The effect can be mitigated, at the expense of light intensity, by placing an integrating sphere ahead of the photodetector. The NIST reference spectrophotometer⁸ employs such an arrangement.

The "inverted" geometry of Fig. 1b is necessary for simultaneous (parallel) detection of many wavelengths. Broadband light is passed first through the sample and then dispersed onto the array detector. A similar potential for beam deflection error exists as for the normal geometry. However, it is now the uniformity of the illuminating source that determines the measurement bias for a given beam deflection rather than the detector, since the beam deflection causes a different portion of the source to be imaged onto the spectrometer slit. Since the slit and active source regions are typically smaller than the detector face in normal geometry, small geometric changes in the beam may be more important.

Convergent and Collimated Sample Beams. Figure 2 illustrates two limiting sample beam geometric configurations that may be used with either of the two instrument configurations discussed above. For a normal instrument, the "source" in Fig. 2 represents the output slit of the source/monochromator combination, while for an inverted instrument, the "detector" actually represents the input slit of the optical multichannel analyzer.

In the geometry commonly referred to as "convergent beam" and illustrated in part a of the figure, the image of the source is relayed first to the central plane of the sample location and then to the input plane of the detector. Unit magnification and equal focal lengths are shown for simplicity. Also, reflective optics may be employed instead of the lenses shown in the illustration. The exact focal plane of the second image may be displaced from the detector entry plane by inserting a sample of finite thickness and typical index of refraction. If the instrument is focused for a particular sample size and typical index, it will be out of focus when a long cell or thin solid standard is in place. This focus-shifting effect has more serious consequences for an inverted instrument with a slit at the desired focus than for a conventional instrument with a large detector face at the focus. As it passes through the sample, the beam is approximately the size of the source filament, cavity, or slit, so will typically underfill the sample cell windows without masking.

Part b of Fig. 2 illustrates "collimated beam" geometry, again with a lens pair for illustration, and equal focal lengths for simplicity. The collimated beam in which the sample is inserted is radiometrically preferred for absorption, since all optical rays traverse the same distance through the sample, unlike the convergent geometry. Indeed "regular transmittance" is defined with respect to a collimated beam, and bias corrections and/or uncertainty components should be included for convergent beam instruments. However, the collimated beam may overfill practical sample cells and require aperturing for both reference and sample measurements, thus reducing the effective source intensity. The optical pathlength of the sample has no effect on the final focal plane of the source as imaged on the detector plane.

Effect of Optical Wedge in the Sample. Figure 3 illustrates the deflection of a collimated beam of light in-

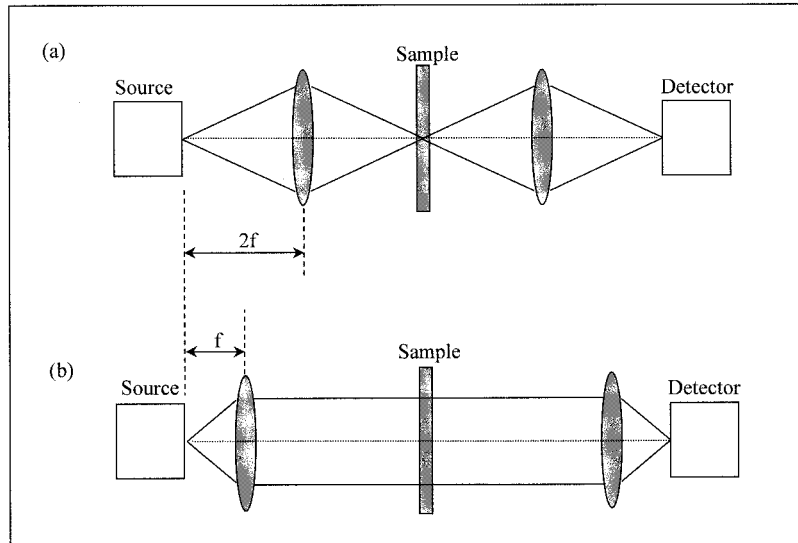


FIG. 2. Two limiting sample beam geometric configurations that may be used with either of the two instrument configurations of Fig. 1. (a) "Convergent beam" geometry and (b) "collimated beam" geometry.

cident on an optical window whose entry and exit faces are optically flat but form a wedge angle of δw between them. Actual wedge angles of interest are on the order of a milliradian and thus much smaller than illustrated in the figure. For ease of computation, consider the light to be normal to the entry surface and thus incident upon the interior of the exit surface at the wedge angle. The relationship between the angles at the exit face and the indices of refraction of the two media is given by Snell's law as

$$n \sin(\delta w) = \sin(\alpha + \delta w) \quad (2)$$

where α is the angle of deflection of the original incident beam, n is the index of refraction of the window, and the index of refraction of air is approximated as unity for simplicity. For small angles,

$$\alpha \cong (n - 1)\delta w \quad (3)$$

and the deflection angle can be seen to be about half the wedge angle for a typical index of $n \cong 1.5$.

About 4% of the incident light is back-reflected from each surface. The entry face of the window in Fig. 3 will produce a back-reflection coincident with the incident beam. The exit face will produce a back-reflection that is incident on the interior of the entrance face at an angle of $2\delta w$. Snell's law at small angles then reveals that the back-reflection angle β , relative to the normal to the entry face, is given by

$$\beta \cong 2n\delta w. \quad (4)$$

For reasonably small rotations of the window about normal incidence to the entry face, the angle α serves as a good approximation to the forward deflection due to the wedge in the window, and the angle β serves as a good approximation to the angle between the back-reflections from the two faces of a wedged window. These angles form the basis for the optical measurement of the wedge in an optical element.

Determination of Optical Wedge in Solid Standards. Basic ray-tracing optics may be used to demon-

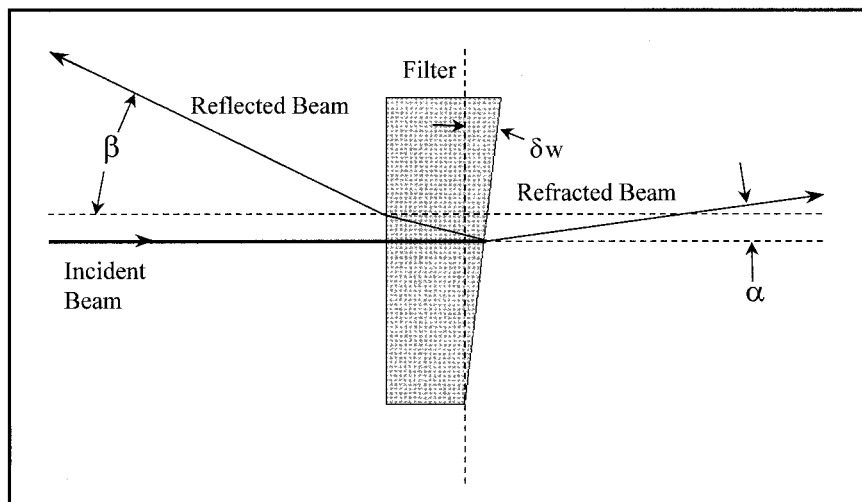


FIG. 3. The deflection and second-surface reflection of a collimated beam of light normally incident on an optical window whose entry and exit faces are optically flat but form a wedge angle of δw between them.

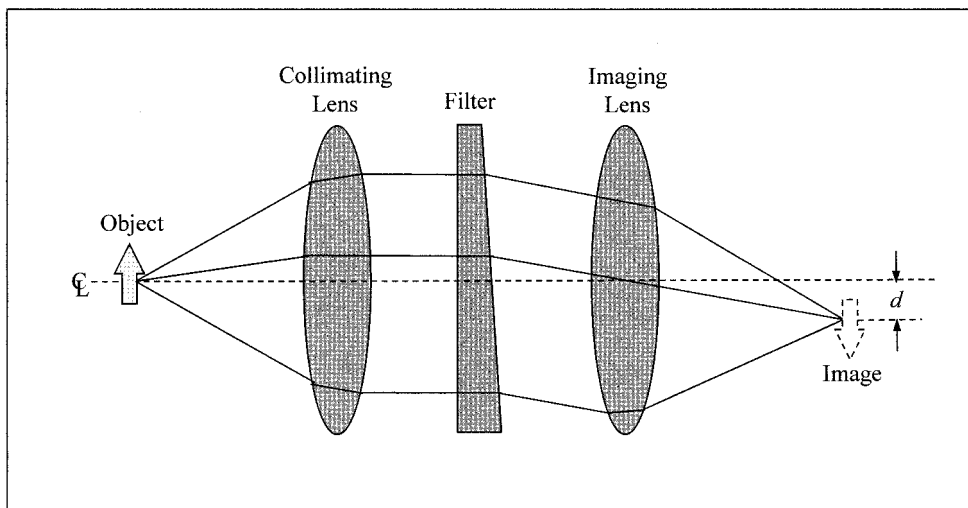


FIG. 4. Image displacement by a wedged sample in a collimated beam.

strate that the convergent and collimated beam optics of Fig. 2 differ dramatically in their sensitivity to tilt (angular displacement of the average surface normal from the optical axis) and wedge in the sample. In fact, the former is sensitive to tilt but not wedge, while the latter is sensitive to wedge and not tilt, at least to the first order in both cases. The sensitivity of the collimated beam geometry to angular deflection of the beam is, in fact, the basis for the design of the classical optical autocollimator.

The design principles of an autocollimator are shown in Fig. 4. Note the similarity to Fig. 2b, but here the "source" is now characterized as the "object", which gives rise to an "image" at the far focal plane. The image is shifted by a distance d in the image plane, resulting from a deflection by an angle α in the collimated beam (such as caused by the wedge in an intermediate window, as shown in Fig. 3.) Since the image plane is a distance f from the imaging lens, where f is the focal length of that lens, then the unrefracted ray passing through the center of the lens may be used to characterize the offset distance d as

$$d = f \tan(\alpha) \cong f \sin(\alpha) \cong f\alpha, \quad \alpha \ll 1. \quad (5)$$

In practice, the object may be a back-illuminated reticle or set of crosshairs, and the image plane may contain a corresponding structure mounted to one or two calibrated micrometers, to measure one or both components of d along two orthogonal axes of the image plane. For a typical focal length of 300 mm, a deflection angle of 0.3 mrad (or $1'$) gives a displacement of 90 μm , easily compatible with typical micrometers.

The lenses shown in Fig. 4 may be thought of as the objective lenses of a collimator and a telescope. Each instrument may have an additional condensing or eyepiece lens, which is not illustrated here for simplicity. The autocollimator is designed for use with an external reflector, whose return beam may be deflected from the projected beam by a small angle, and folds the function of the two telescopes into one. The conventional design combines the function of the two instruments by using a single objective lens, with a beamsplitter behind this objective lens to separate the "transmitting" and "receiving" functions.

The autocollimator may be used to determine the wedge in a clear window by measuring the differential angle between the return beams reflected from the entry and exit faces of the window. For solid absorbing filters, however, the back-reflection from the far surface is too attenuated for observation, and the transmitting "collimator/telescope" configuration is required. Unfortunately, the observation of the angle α instead of the angle β results in a sixfold loss of wedge measurement sensitivity for $n \cong 1.5$, as may be seen from Eqs. 3 and 4.

Wedge Tolerance for Solid Standards. The calculation given above for characterizing the operation of an autocollimator may be used to model the effect of optical wedge in a collimated-beam spectrophotometer. The 90 μm deflection for the example given may be compared with typical spectrophotometer slit widths to determine the potential for measurement error. For an inverted geometry instrument with a photodiode array detector with 25 μm pixel spacing and 1:1 imaging of the entrance slit on the detector plane, a slit width of 25 μm can be inferred. Thus a 0.3 mrad deflection would cause a displacement by three and a half slit widths for a 300 mm imaging lens.

However, in a spectrophotometer one would minimize the focal length of the imaging lens to minimize the deflection. Hence, a more typical focal length for the spectrophotometer may be 30 mm, reducing the displacement to a third of a slit width for a 0.3 mrad deflection. Thus, a 0.05 mrad ($10''$) deflection would correspond to about 6% of a slit width, and to a wedge angle of 0.1 mrad ($20''$) in the optical element, as shown in Eq. 3 above. NIST has chosen this wedge angle, somewhat arbitrarily, as the maximum tolerance for wedge in solid filters. This is a compromise between the desired ideal and production realities. The NIST wedge tolerance applies specifically to wedge along the short axis of the solid filter (transverse wedge), which would give rise to deflection across the entrance slit. Wedge along the long axis of the filter is—for now at least—neither considered nor usually measured.

The bias resulting from an array detector viewing a rectangular segment of the source that is displaced by 6%

of the viewing field is not predictable without prior knowledge of the uniformity of the source. However, if one makes the rational assumption that a particular shift in the viewing field could result in a given *relative* error in the background measurement—and hence the measured transmittance—then Eq. 1 implies that the error in absorbance units would be independent of the actual absorbance of the sample or standard causing the deflection.

EXPERIMENTAL

Inverted Geometry Spectrophotometer. The Hewlett-Packard 8453† is a compact (measuring just 56 cm in its greatest dimension), inverted geometry spectrophotometer with collimated beam optics. The small footprint is achieved largely through the use of short-focal-length lenses (on the order of 20 to 25 mm in focal length, by visual inspection) for beam collimation and imaging. Since the beam-forming optics are refractive—and not achromatic—the collimation and imaging configuration is a compromise over the 190 to 1100 nm wavelength span of the photodiode array detector. Nevertheless, both lenses are apertured to about 5 mm, and are separated by about 18 cm, requiring a reasonably high degree of collimation to ensure sufficient throughput at all wavelengths. Data are acquired with a 1024-element photodiode array and interpolated in firmware onto a data grid at 1 nm intervals. The optical bandwidth of the instrument is about 1.5 nm. The spectral range and wavelength-multiplexed detection require that both tungsten and deuterium lamps be incident on the sample simultaneously. This goal is achieved by imaging a tungsten lamp into the center plane of a hollow deuterium lamp.

The instrument is equipped with an optional sample transporter accommodating up to seven cuvettes or filters at once. Despite its specified drift rate of less than 0.001 absorbance units per hour after one hour of warm-up, we keep an empty filter holder in one of the seven positions and run a new “blank” or background before each sample. With a typical integration time of 0.5 s, acquisition of the background and sample spectra is complete in less than 30 s, including multiple exposures for baseline and scatter correction, data transfer time, and sample/blank transport time. Some of the data for this paper—involving difference absorbances with samples reversed—were taken in a different, but closely related, manner. Such difference spectra may be obtained with the sample in normal orientation as the “blank” and the reversed sample as the “sample”. Again, the two runs may be accomplished within 30 s, minimizing the opportunity for source drift in the single beam instrument.

Autocollimator Pair. Wedge angles are measured optically with a pair of Gaertner M551 autocollimators, set up facing each other on an optical rail, with a sample holder in between. One autocollimator is used as the collimated source, projecting a back-illuminated reticle into the other autocollimator, used as the telescope/receiver.

A small charge-coupled device (CCD) camera has been adapted to the eyepiece of the receiver, and the image of the reticle is displayed on a monitor along with the image of the receiver reticle.

The autocollimators are each equipped with a single micrometer, which translates the reticle in a calibrated and reproducible fashion in one dimension. The objective focal length of the M551 is 250 mm, giving a displacement of 250 μm per mrad of beam displacement. The linear micrometers are calibrated to yield a response of approximately one division on the micrometer drum per 5 μrad ($1''$) of deviation from normal of an external reflector. Several potentially confusing factors of 2 are associated with relating the calibration as defined for the autocollimator in reflection to one associated with detection of wedge in transmission with two instruments: (1) The deviation angle between the exiting and returning beam in an autocollimator is twice the deviation from normal of the external reflector. (2) The Gaertner design uses a single reticle for both projection and detection, so that the inverted image upon reflection moves in the opposite direction to the directly viewed reticle as the micrometer is turned. (3) For the transmission measurement, the deflection angle is approximately half of the wedge angle, as shown above.

Since the direction of beam deflection is inverted when the wedged filter is reversed, we take the difference in the two micrometer readings for the two orientations of the filter. We have calibrated the difference micrometer reading against a precision comparator—as described below—and found the true optical wedge to be about 11 μrad (2.2'') per micrometer division.

Since the autocollimators are equipped with micrometer translation in only one dimension, the wedge component along the short axis of the filter (transverse wedge) is normally read, and the 0.1 mrad tolerance is applied to this axis only, yielding the deflection component to which spectrophotometers are most sensitive. The sample holder has been designed, however, so that it may be rotated by $\pi/2$, yielding the wedge along the long axis of the filter.

Comparator Measurements. The glass and fused-silica optical filter standards are fortuitously similar in dimension to gage blocks used in precision engineering. The thickness of such gage blocks is routinely determined to accuracies of a few nanometers with mechanical comparators. An Esterline Federal Comparator in the Precision Engineering Division of NIST was employed to measure the transverse wedge of a suite of five optical filters.⁹ For this purpose, two measurements were made at a separation of 8 mm, with a measurement uncertainty of about 0.1 mm determined by the translation stage employed. A wedge of 1 mrad may be shown to correspond to a thickness difference of $\sim 8 \mu\text{m}$ at this separation with the wedge measurement uncertainty dominated by the 1:80 relative uncertainty of the abscissa. At 0.05 mrad, the thickness difference of about 400 nm would result in an uncertainty contribution from the ordinate of about half that of the abscissa. This uncertainty is still small compared to that of the optical system being calibrated.

Standard Reference Materials. NIST SRM 930, “Glass Filters for Spectrophotometry”, has been issued since 1971. The SRM contains three filters of 10, 20, and

† To describe experimental procedures adequately, it is occasionally necessary to identify commercial products by manufacturer's name or label. In no instance does such identification imply endorsement by the National Institute of Standards and Technology, nor does it imply that the particular products or equipment is necessarily the best available for that purpose.

TABLE I. NIST solid photometric standards.

SRM	$T_{\text{nom}}/\%$	Td_{nom}^a	Material ^b	t mm ^c	(Wave-lengths of certification)/nm
930	10	1.00	NG-4	1.89	440,465,546.1, 590,635
	20	0.70	NG-4	1.31	
	30	0.52	NG-5	1.91	
1930	1	2.00	NG-3	2.01	
	3	1.52	NG-3	1.50	
	50	0.30	NG-11	2.27	
2031	10	1.00	Fused	2×1.5^d	250, 280, 340, 360, 400, 465, 500, 546.1, 590, 635
	30	0.52	Silica	2×1.5^d	
	90	0.05		3.0	

^a Nominal transmittance density (unitless).

^b NG glasses are from Schott Glass Technologies, Duryea, PA; fused silica is from Dynasil, Berlin, NJ.

^c Plate thickness. SRM 930 and SRM 1930 are ground to ± 0.02 mm; SRM 2031 to ± 0.1 mm.

^d Cr film is evaporated onto one plate, and a cover plate is optically contacted.

30% nominal transmittance in the visible spectral range and an empty filter holder to be used for the background measurement. The filters are ground from Schott NG series glasses to a flatness of <633 nm over the central 5 mm by 20 mm area, to the dimensions given in Table I. The transmittances are individually certified with the reference spectrophotometer at the five visible wavelengths indicated in the table. Consecutive batches of SRM 930 were offered as series designations 930, 930a, 930b, 930c, and 930d, until it was determined that the batch differences were inconsequential, and the series designation remained at SRM 930d for a number of years. The recent change in series designation to SRM 930e reflects the tightening in optical wedge tolerance, and the individual determination of the optical wedge on certified filters, as reported here.

NIST SRM 1930 also contains three filters of 1, 3, and 50% nominal transmittance, extending the range of SRM 930 in both directions. The source glasses and thicknesses used for these filters are also shown in Table I. Glass

for this SRM is now being ground to the same specifications as SRM 930e, and the new SRM 1930a with improved wedge specifications will become available in 1999.

NIST SRM 2031 extends the measurement range of solid filter standards into the UV, as shown in Table I. All three filters of the set are based upon fused silica, with good UV transmission. Filters of nominal 10 and 30% transmittance are obtained with thin evaporative coatings of chromium; the nominal 90% transmittance filter is uncoated, reflecting about 4% of the incident light from each uncoated surface. Though the light attenuation mechanism is different from the absorptive filters of SRMs 930 and 1930, SRM 2031 requires the same attention to optical wedge, and the substrates and cover plates for SRM 2031a are ground to the same tolerances as SRM 930e.

NIST SRM 2034 is used for the calibration of the wavelength scale of UV-visible spectrophotometers, and consists of an aqueous solution of 4% (mass fraction) holmium oxide in 10% (volume fraction) perchloric acid, sealed in a fused-silica cuvette. Fourteen spectral bands are certified for their position of minimum transmittance over a spectral range from 240 nm to 650 nm, with an expanded uncertainty of ± 0.1 nm. High-quality commercial cuvettes used for the standard are specified as accurate to ± 10 μm in pathlength, flat to less than 1.3 μm , and with entry and exit faces parallel to ~ 0.9 mrad (3 $^\circ$).

Cuvettes. Seven 10 mm pathlength cuvettes with screw-on caps were obtained from each of two vendors. The optical specifications were identical to those given above for the cuvettes of SRM 2034.

RESULTS

Comparison of Optical and Mechanical Measurements. Figure 5 shows the result of calibrating the optical wedge measurement system against the precision mechanical comparator. The indicated uncertainties for the comparator are based upon an estimated uncertainty of

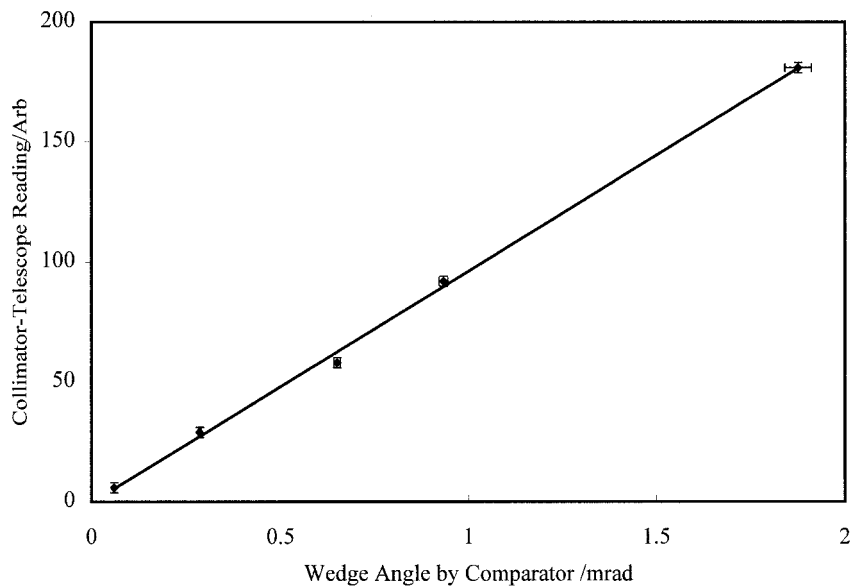


FIG. 5. Optical vs. physical wedge measurement for five filters.

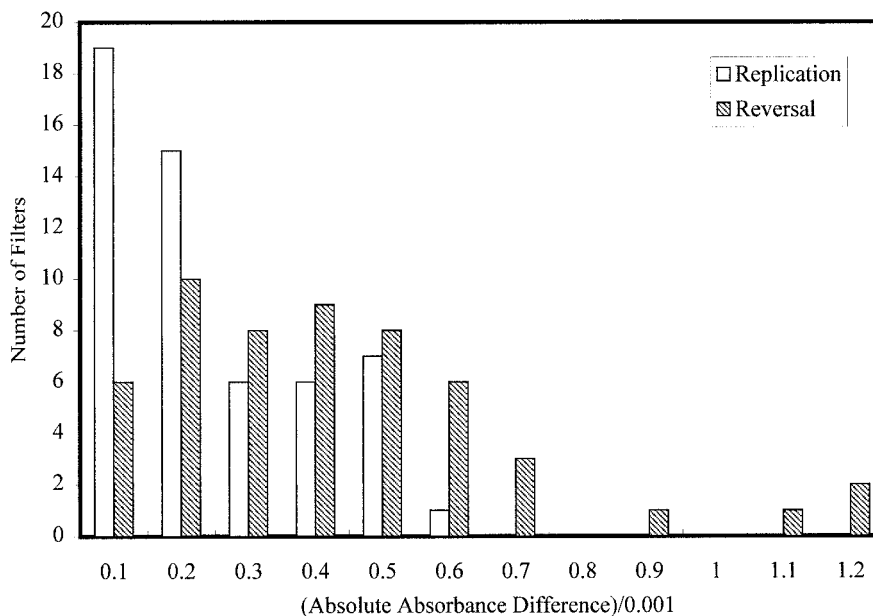


FIG. 6. Population distributions of reversal and replication absorbance differences for 54 production filters, for a 31 nm wavelength band about 530 nm.

0.1 mm in determining the separation of the two positions at which the filter thickness was determined. For the lower four wedge values, the two positions were 8 mm apart, and the relative uncertainty of 1:80 is indicated in the figure. For the highest wedge, the two points were 5.3 mm apart, because of the range limit of the comparator, and a relative uncertainty of 1:53 is indicated. The indicated uncertainties of ± 2.13 micrometer divisions for the optical measurement represent twice the estimated pooled standard deviation of three replicate readings from each of 36 filters, for a total of 72 degrees of freedom.

The reciprocal of the slope of a linear fit yields a calibration of approximately 0.0105 mrad per micrometer division, for an expanded uncertainty of $\pm(2.13 \times 0.0105)$ mrad or ± 0.022 mrad for our optical method. Thus, the autocollimator system is capable of detecting samples that exceed our target specification of 0.1 mrad ($20''$) of wedge.

Wedge Effects for Solid Photometric Standards for Inverted Geometry. A useful diagnostic for detecting effects due to optical wedge is to examine the effect of reversing the filter. Reversing the filter reverses the deflection, so that the translation of the field of view is twice that of simply inserting the filter and comparing it to an "air" background. Furthermore, the difference spectrum between the two orientations is unaffected by the true absorption in the glass, leaving only the result of the beam deflection artifact in the resultant spectrum. Unfortunately, the shift in the field of view is coupled with the homogeneity of the source to influence the apparent absorbance. For a perfectly homogeneous source, beam deflection would not be expected to yield an absorbance change. Also, for a source with a symmetrical intensity profile, and with the true optical axis aligned to the maximum of the profile, filter reversal could yield a null difference due to symmetry instead of the absence of wedge.

A 31 nm band of wavelengths from 515 to 545 nm

was used as a simple diagnostic to evaluate the effect of wedge on absorbance for a current production run of 18 sets of SRM 930e and for our particular instrument. The use of a sum of 31 adjacent spectral points reduces the random uncertainty by approximately $31^{1/2}$. Each of the 54 filters in the 18 sets of 10, 20, and 30% filters was run three times, with removal and replacement. The filter was run facing the normal direction, the reverse direction, and then the normal direction again. Figure 6 shows a histogram generated from these data. One set of bars ("replication") depicts the distribution of the absolute differences for the filter facing in the normal direction and is thus a measure of the precision of the experiment. The second set of bars ("reversal") depicts the distribution of the absolute differences for the filter facing in opposite directions. The second distribution may be seen to be expanded somewhat beyond the first, indicating some small effect of optical wedge. The entire distribution is well within the expanded uncertainty limits for the SRM, though it well may differ for different instruments from the same assembly line.

Fortunately, filter reversal provides a more reliable diagnostic of wedge than simply the result of shifting the field of view of the spectrometer slit. Figure 7 shows absorbance difference spectra obtained for three nominal 30% transmitting neutral glass filters, which were also used in the calibration exercise of Fig. 5. (The optical wedge values given are those determined by the mechanical comparator.) The most striking features have much more spectral character than could be expected from a simple translation of the field of view. Indeed, the features at 486.0 and 656.1 nm correspond to well-known lines from the system deuterium lamp and result from an apparent *spectral* shift caused by the small change in beam entry *angle* into the spectrometer. Thus, the spectral axis is shifted slightly between the two spectra being subtracted, and the spectral lines yield a differential pattern approximating the shape of the first derivative of the line.

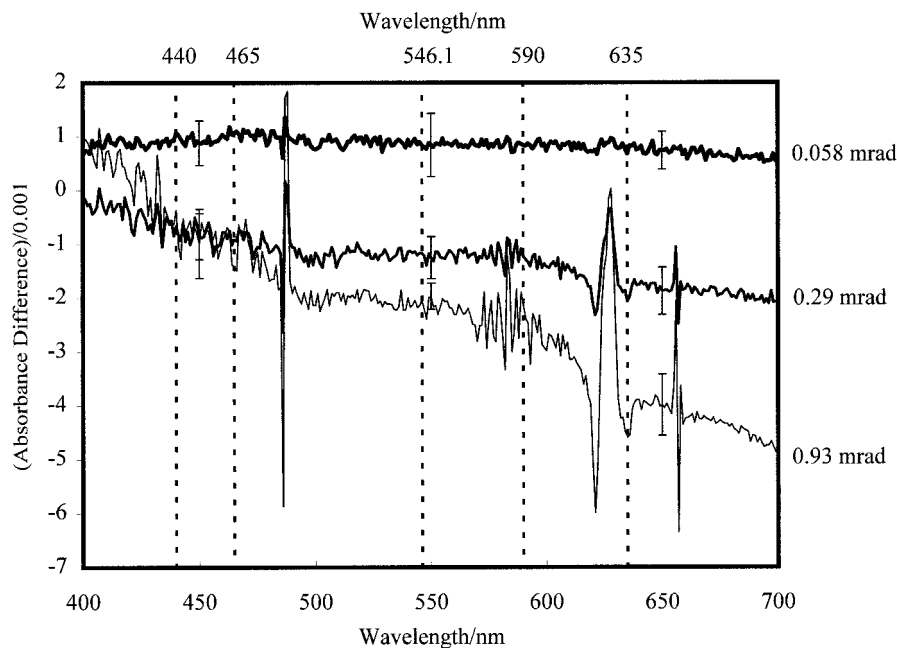


FIG. 7. Absorbance effect of filter reversal as a function of wavelength and wedge, for three nominal 30% transmitting neutral glass filters. Also indicated on the figure are the five wavelengths at which SRMs 930 and 1930 are certified (dashed lines).

The deuterium lamp is not essential for measuring visible spectra, but improves the signal-to-noise ratio at the blue end of the spectrum and thus is normally kept on. When the data of Fig. 7 are re-acquired with the deuterium lamp off, the spectral features at 486.0 and 656.1 nm disappear, as well as the "hash" in the region of 570 to 600 nm. The feature in the 620 to 640 nm region remains, however, and so may be attributed to any of a number of other instrumental components such as the visible lamp, the grating, or the stray light correction filter.

Uncertainties shown in the figure for three of the 301 wavelengths for each of the filters are 95% confidence intervals derived from six measurements of each filter; three with the filter turned in one direction and three in the other. The expansion factor from Student's t distribution is 2.78 for four degrees of freedom (two for each of the two averages of three spectra used in the difference) and 95% confidence. Because the sharp features are statistically indistinguishable for the 0.058 mrad wedge data, it is unclear that the sign of these data is consistent with the other two data sets, which may be "signed" by matching the polarity of the features.

Sealed Wavelength Standard Cuvettes. The bottom curve of Fig. 8 (right-hand ordinate axis) shows the transmittance density spectrum of a cell of SRM 2034 with an apparent wedge of ~ 0.63 mrad ($2' 10''$) determined optically. The trace is the average of two runs taken before and after reversal of the cell. The middle trace is the difference of the same two runs, and shows numerous spectral artifacts that result both from spectral features in the measurement system and from the shift in the spectral features of the absorbing solution upon cell reversal. Finally, the top trace is a reversal trace using a reject SRM 2031-30% metal-on-fused-silica neutral filter with an optically determined wedge of about 0.58 mrad ($2'$), shown to distinguish the spectral features of the measurement system from those of the wavelength standard. Both of

the reversal difference spectra relate to the left-hand ordinate axis of the figure.

A crude calibration of the wavelength shift may be obtained with an approximate numerical first derivative of the spectrum by using differences of adjacent channels. The spectral features of this derivative are similar to those in the difference spectrum, but about 100 times larger. This observation implies a spectral shift on the order of 0.01 nm for reversal of the 0.63 mrad-wedged-cuvette. For a single spectrum referred to air, the shift would be half as great, and for the maximum wedge of 0.9 mrad ($3'$) for SRM 2034 the shift would be less than 0.01 nm. This value is well below the certified uncertainty of 0.1 nm for all of the 14 bands and of no consequence for practical spectrophotometry.

Figure 9 illustrates a more sophisticated approach to the spectral shift caused by wedged cells of SRM 2034. Three cells of the standard were run three times in each of the two orientations, and the GRAMS/32 spectral analysis program (Galactic Industries, Salem, NH) was used to locate the positions of all 14 certified bands. The figure shows the shift in apparent peak position as a function of optically determined cell wedge for 5 of the 14 certified bands. The uncertainty limits are again 95% confidence intervals for 3 degrees of freedom for the ordinate and 72 degrees of freedom for the abscissa.

The observed shifts are consistent in general with the above estimate with the numerical first derivative, but the band-to-band difference indicates that peak picking may be influenced by the shape and width of a particular band as well as the shift in the underlying axis. Logically, all the curves should extrapolate through the origin, and yet only a few appear to do so. The 361.1 nm band showing an inverted slope may be seen in Fig. 8 to be closely coincident with one of the spectral features native to the instrument, and thus the peak-picker is locating the max-

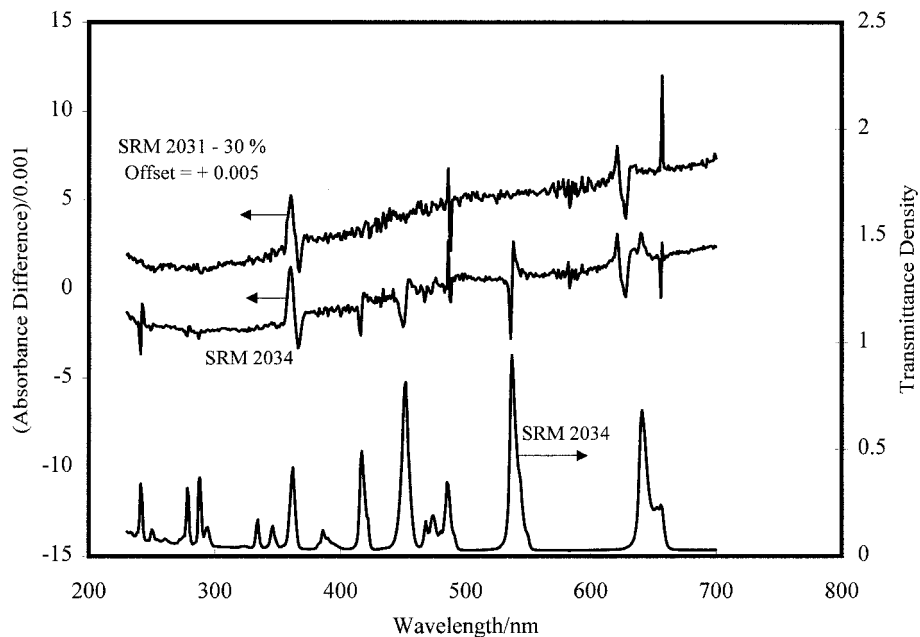


FIG. 8. Spectral artifacts introduced by a sample of SRM 2034 with a wedge of 0.63 mrad may be seen in the filter-reversal absorbance difference spectrum in the center trace for comparison with the spectrum of the standard in the lower trace. The upper trace is the reversal absorbance difference spectrum of a reject SRM 2031-30 filter of similar wedge, offset by +0.005 AU for clarity and is included to illustrate the spectral artifacts arising from other components in the system, and *not* SRM 2034.

imum of the standard confounded with an artifact spectral feature.

Liquid-filled Cuvettes. The commercial cuvettes were tested (with the autocollimator pair) empty, filled with water, and filled with methanol. The cuvettes from one manufacturer showed no detectable wedge when measured empty and a maximum apparent wedge of 0.33 mrad when filled with water. The cuvettes from another source showed appreciable wedge for almost all samples, with similar values for the empty, water-filled, and meth-

anol-filled cells. The largest apparent wedge was on the order of 5 mrad, almost beyond the range of measurement, and well over the expected maximum of 0.9 mrad.

Wedge measured for an empty cell results from the combined wedge in the two windows and could fortuitously cancel if two similarly wedged faces are oriented with the wedge in opposite directions. However, it is more likely that low wedge readings imply low wedges in the fused-silica components used. When the cell is filled with a liquid whose index of refraction exactly

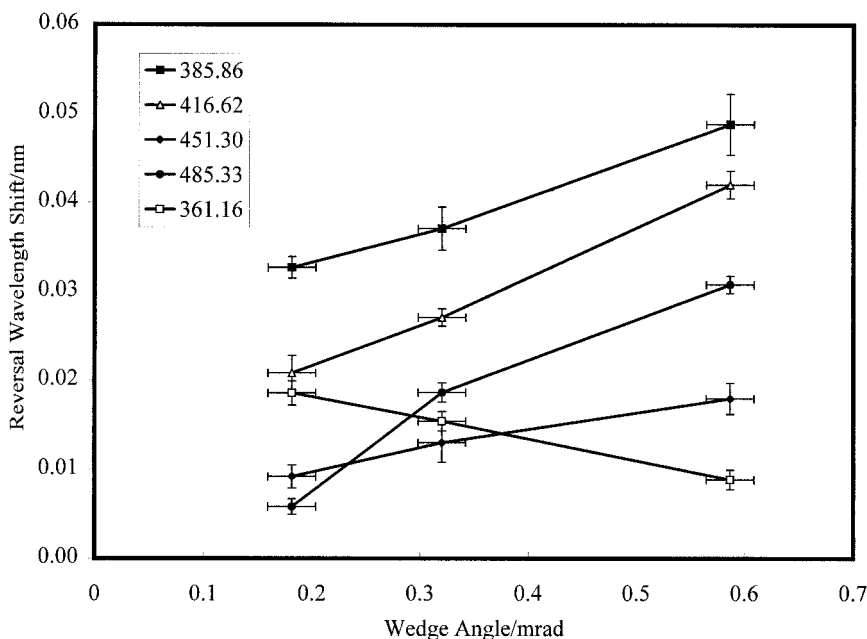


FIG. 9. Apparent peak position shift with cell reversal as a function of cuvette wedge angle for five of the fourteen certified bands in three cells of SRM 2034.

matches that of fused silica, the measured wedge is strictly a measure of the parallelism of the entry and exit faces of the cuvette. If the index of refraction of the fill medium differs appreciably from that of fused silica, the "apparent wedge" as we have referred to it above is a more complicated function of various possible contributions.

One of the cells from the source with generally poor performance could not be read on the autocollimator pair. The optical quality of the cell was so poor that the image of the reticle that had passed through the cell could not be refocused by the imaging objective lens of the receiving autocollimator. This effect is referred to as "dispersion" in an excellent, brief tutorial on cell performance by "The Cell Working Party" of the British "UV Spectrometry Group"¹⁰ and should not be confused with spectral dispersion resulting from a grating or prism. The tutorial provides a simple diagnostic setup to examine cells for both angular deviation and dispersion.

DISCUSSION

Inverted geometry spectrophotometers with collimated beam optics are particularly sensitive to the effects of optical wedge in sample cuvettes or solid standards. The purely photometric effect due to changes in the effective field of view of the entrance slit of the optical spectrometer turns out to be a less sensitive and robust indicator of optical wedge problems than the appearance of spectral artifacts resulting from slight wavelength shifts. These artifacts are entirely independent of source heterogeneity and make it straightforward to diagnose the presence of unacceptable wedge in standards and sample cells.

In the case of solid standards referred to air, it is especially important that the apparent wedge be kept to approximately 0.1 mrad or less for use with collimated-beam, inverted-geometry instruments. Some NIST standards produced before 1996 exceed this wedge tolerance and may yield questionable verification results on such instruments. NIST recommends the filter reversal test to diagnose the behavior of filters on these instruments. NIST will replace solid filters produced after 1995 for which any part of the reversal difference spectrum from 440 nm (or 250 nm for SRM 2031) to 635 nm falls outside the expanded uncertainty range for that filter (nominally ± 0.002 absorbance units for SRM 930). (Referring to Fig. 7, the filter for which the wedge is given as 0.29 mrad would qualify for replacement since features at 486 nm and 622 nm extend below -0.002 absorbance units.) If older filters are found to have unacceptable wedge, it is recommended that new filters be ordered.

It may be seen from Fig. 7 that the certification wavelength of 635 nm is more adversely affected by the accidental coincidence with a spectral artifact than any of the other certification wavelengths for SRM 930 and SRM 1930. For some older standards, the filter reversal test may reveal satisfactory performance for four of the five certified wavelengths.

For the sealed wavelength standard, SRM 2034, the apparent wavelength shifts produced by cells wedged at the maximum specification of 0.9 mrad or less are small with respect to the expanded uncertainty given for the certified wavelengths (0.1 nm). However, if the cell re-

versal difference absorbance spectrum is appreciably worse than shown in Fig. 8, the cell may be out of specification and NIST should be consulted.

Optical wedge and poor optical quality or dispersion are of concern for routine chemical operation with reusable cuvettes. The highest degree of spectrophotometric accuracy is achieved by using the same cell in the same orientation for both the background and sample measurements, without removing the cell from the instrument (pipetting the blank and sample solutions into and out of the cell with multiple rinses). Only slightly less accurate is the use of the same cell and orientation *with* cell removal and replacement. Thus, it is advantageous to mark cells both for identification and for the ability to orient them the same way with each use. Either way, the effects of wedge and dispersion effectively cancel in the ratio represented by the transmittance (for comparable refractive index in the blank and in the sample).

Alternatively, cells to be used with a wedge-sensitive instrument may be preselected with cell reversal difference spectra, an autocollimator (or the version illustrated by The Cell Working Group¹⁰), or a laser. The laser method is simpler than the autocollimator and is probably less sensitive to dispersion than the autocollimator because of the small spot size. To measure optical beam deflection with a laser, one would set up a laser a few meters from a screen, mark the position of the undeflected laser spot on the screen, insert the sample cell normal to the beam (using the retro-reflected beam for alignment), and measure the resulting deflection of the laser spot. The deflection angle is then the arctangent of the deflection divided by the distance from the screen to the cell.

CONCLUSION

In a collimated-beam spectrophotometer, the sample beam is deflected by about half of the wedge angle present in the sample. This deflection has particularly serious consequences for an inverted-geometry instrument, since small deflections can equate to large changes in the field of view at the entrance slit of the spectrometer downstream from the sample. In addition to the direct photometric consequences of the changing field of view, beam deflection is found to induce small apparent wavelength shifts in data taken through a wedged sample. This shift results in artifacts deriving from spectral features of the spectrophotometric system itself or from spectral features of a well-resolved absorbing sample. These spectral artifacts turn out to be robust and useful diagnostic indicators of sample wedge using reasonably simple cell-reversal difference spectra.

Solid photometric standards for spectrophotometry should be reliable for both instrument configurations, if held to wedge angles of less than about 0.1 mrad. Despite a wedge tolerance of 0.9 mrad in the sealed cuvettes of the SRM 2034 holmium oxide wavelength standard, wavelength shifts are shown to be negligible with respect to the uncertainties given for the certified spectral bands.

Since commercial cuvettes may vary widely in optical quality, several methods have been described to check the optical quality. Alternatively, accuracy may be maintained by utilizing the same cell in the same orientation for background and sample spectra, thereby canceling ef-

fects due to wedge or dispersion when the index of refraction is comparable for the blank and the sample.

ACKNOWLEDGMENTS

The authors are especially grateful to Beno Mueller, of Hewlett-Packard GmbH, for identifying the optical wedge problem and recommending tightened tolerances for SRM 930; to Thomas Germer of the NIST Optical Technology Division for first diagnosing the spectral shift artifacts; to Eric Stanfield of the NIST Precision Metrology Division for the comparator measurements; to Mary Smeller of the NIST Analytical Chemistry Division for helpful data acquisition; and to Michael Winchester, Marc Salit, and Pamela Chu of the Analytical Chemistry Division for many helpful discussions.

-
1. R. Mavrodineanu, in *Solid Materials to Check the Photometric Scale of Spectrophotometers*, O. Menis and J. I. Shultz, Eds. (U.S.

- Government Printing Office, Washington, D.C., 1970), NBS Tech. Note 544.
2. R. Mavrodineanu, *J. Res. Natl. Bur. Stand. (U.S.)* **80A**, 637 (1976).
3. R. W. Burke, E. R. Deardorff, and O. J. Menis, *J. Res. Natl. Bur. Stand. (U.S.)* **76A**, 469 (1972).
4. R. W. Burke and R. Mavrodineanu, *J. Res. Natl. Bur. Stand. (U.S.)* **80A**, 631 (1976).
5. V. R. Weidner, R. Mavrodineanu, K. D. Mielenz, R. A. Velapoldi, K. L. Eckerle, and B. Adams, *Holmium Oxide Solution Wavelength Standard from 240 to 640 nm—SRM 2034* (U.S. Government Printing Office, Washington, D.C., 1986), NBS Spec. Pub. 260-102.
6. B. Mueller, Hewlett-Packard GmbH, Waldbronn, Germany, private communication (1992).
7. K. D. Mielenz, *Anal. Chem.* **48**, 1093 (1976).
8. R. Mavrodineanu, *J. Res. Natl. Bur. Stand. (U.S.)* **76A**, 405 (1972).
9. E. Stanfield, Precision Engineering Division, National Institute of Standards and Technology, Gaithersburg, Maryland, private communication (1997).
10. C. Burgess and A. Knowles, *Standards in Absorption Spectrometry* (Chapman and Hall, London, 1981), pp. 128-129.